

IFUSP/P-69

"LOW TEMPERATURE DIFFERENTIAL MAGNETIZATION OF  
 $\text{Ni}(\text{ClO}_4)_2 \cdot 6\text{NH}_3$  AND  $\text{Ni}(\text{BF}_4)_2 \cdot 6\text{NH}_3$ " \*

by

A. Paduan Filho            and            N. F. Oliveira Jr.  
Instituto de Física, Universidade de S. Paulo -  
Caixa Postal 20516 - São Paulo, S. Paulo, Brasil

**B.I.F. - USP**

DEZEMBRO/1975

LOW TEMPERATURE DIFFERENTIAL MAGNETIZATION

OF  $\text{Ni}(\text{ClO}_4)_2 \cdot 6\text{NH}_3$  AND  $\text{Ni}(\text{BF}_4)_2 \cdot 6\text{NH}_3$ \*

by

A. Paduan Filho and N.F. Oliveira Jr.

Instituto de Física da Universidade de S. Paulo, C.P. 20516

S. Paulo, S.P., Brasil

ABSTRACT

The differential magnetization of  $\text{Ni}(\text{ClO}_4)_2 \cdot 6\text{NH}_3$  and  $\text{Ni}(\text{BF}_4)_2 \cdot 6\text{NH}_3$  was measured as a function of temperature (20 K to 0.3 K) and magnetic field (up to 40 kOe). An antiferromagnetic transition was found at  $T_N = 0.45$  K for the  $\text{Ni}(\text{ClO}_4)_2 \cdot 6\text{NH}_3$  and  $T_N = 0.43$  K for the  $\text{Ni}(\text{BF}_4)_2 \cdot 6\text{NH}_3$ , and a portion of the magnetic phase diagram was determined. The interpretation of the data in terms of a uniaxial model yielded  $(D/k) \sim 0.2$  K for both salts.

---

\* Work partially supported by CNPq, FINEP and BNDE.  
To be published in J.Phys. and Chem. of Solids

## INTRODUCTION

Cubic salts with chemical formula  $\text{MeX}_2\cdot 6\text{NH}_3$  have been the subject of systematic thermal and magnetic investigations for two principal reasons: hindered rotations of the  $\text{NH}_3$  molecules (1-5) and an antiferromagnetic transition which occurs at low temperatures, when  $\text{Me}^{++}$  is a magnetic ion (Ni, Mn, Co or Fe) (6-10). In these salts, the six triangular  $\text{NH}_3$  molecules occupy the vertices of a regular octahedron around the  $\text{Me}^{++}$  ions which are disposed in a f.c.c. lattice with parameter  $\underline{a} \sim 10\text{-}11.5 \text{ \AA}$ . The axes of each octahedron are coincident with the cubic crystallographic axes. The radicals X form a cubic array of parameter  $\frac{1}{2} \underline{a}$ .

All of the salts mentioned above exhibit a sudden broadening of the EPR line, at a critical temperature  $T_c$ , which has been attributed to the cooperative freezing of rotational degrees of freedom of the  $\text{NH}_3$  molecules (1-3). A theory based on a point charge model was developed by Bates and Stevens (4), to explain this phenomenon. In this theory it was assumed that, above  $T_c$ , the  $\text{NH}_3$  molecules are rotating about the quaternary axes of the octahedron with a frequency much higher than the microwave frequency thus producing an average cubic field on the  $\text{Me}^{++}$  ions. Below  $T_c$ , this rotation is hindered therefore adding a trigonal distortion to the cubic field. For Nickel salts, non-cubic components of the crystalline field, together with the spin-orbit interaction, can lift the degeneracy of the  $\text{Ni}^{++}$  ground spin triplet. The amount of this splitting, measured by the parameter D, has been determined by EPR measurements in diluted salts for the Nickel-Halides and resulted in the relatively low value

$(D/k) \sim 0.4$  K for all three salts (5). Such an anisotropic ground state will have an influence on the magnetic behavior at low temperatures where an antiferromagnetic phase is frequently present (6,7). In particular it may give rise to a spin-flop transition (antiferromagnetic to "canted" phase) and in fact this hypothesis is consistent with the field-dependence of the differential magnetization of the  $\text{Ni}(\text{NO}_3)_2 \cdot 6\text{NH}_3$  (8). In other salts, however, an unusual behavior has been reported which has not yet been understood (9,10).

In this paper we have studied the differential magnetization,  $dM/dH$ , in powdered samples of two salts of the same family,  $\text{Ni}(\text{ClO}_4)_2 \cdot 6\text{NH}_3$  ( $a = 11.41 \text{ \AA}$ ) (11), and  $\text{Ni}(\text{BF}_4)_2 \cdot 6\text{NH}_3$  ( $a = 11.22 \text{ \AA}$ ) (11), as a function of temperature and magnetic field. The temperature range covered (20 K to 0.3 K) allowed the determination of the  $g$ -factor and the Weiss temperature. Both salts exhibited an antiferromagnetic transition below 1 K. From the magnetic field dependence (up to 40 kOe) we could determine part of the magnetic phase diagram and observed an apparent spin-flop transition at about  $H_{\text{SF}} \sim 4-5$  kOe. The discussion of the data in terms of a uniaxial model permitted an estimate of  $D$ , which is compared with other reported data.

## EXPERIMENTAL

The  $dM/dH$  was measured by a Hartshorn bridge similar to that described by Maxwell (12), in a variable temperature cryostat similar to that described by Oliveira and Quadros (13). Here, the only important modification was to place the pick-up coils inside the sample bath to minimize spurious signals coming from

the inhomogeneities of the external magnetic field. This field was produced by a superconducting solenoid.

An uncertainty of about 2% was estimated in the measurement of  $H$  (and this includes demagnetizing factors) and of about 3% in  $dM/dH$ . The calibration of  $dM/dH$  in CGS units was made by comparison with Manganous Ammonium Sulphate. The measurement of  $T$  above 4.2 K was made by means of semiconducting sensors previously calibrated against magnetic thermometers (overall estimated accuracy better than 0.1 K). Below 4.2 K, a carbon resistor together with vapor pressure (estimated accuracy better than 0.01 K) was used.

The  $Ni(ClO_4)_2 \cdot 6NH_3$  was prepared in two steps: - by dissolving Nickelous Carbonate in  $HClO_4$  at  $110^\circ C$ , and cooling down, small crystallites (needles) of  $Ni(ClO_4)_2 \cdot 6H_2O$  were obtained; - then, by adding a solution of  $NH_4OH$  at  $50^\circ C$  and cooling down, the blue octahedric crystallites of  $Ni(ClO_4)_2 \cdot 6NH_3$  were formed. The  $Ni(BF_4)_2 \cdot 6NH_3$  was obtained by dissolving Nickelous Carbonate in  $HF_4$  and adding  $NH_4OH$  at about  $50^\circ C$ . During the cool down, crystallites of  $Ni(BF_4)_2 \cdot 6NH_3$  were formed. Analysis of the  $NH_3$  content were performed on all samples measured.

## RESULTS AND DISCUSSION

Fig. 1 shows  $(dM/dH)^{-1}$  versus  $T$ , for  $H = 0$ , up to 20 K, for both salts. The Curie-Weiss behavior observed above 2 K yields a  $g$ -factor and a Weiss temperature of:  $g = 2.17 \pm 0.01$  and  $\theta = -1.00 \pm 0.1$  K for the  $Ni(ClO_4)_2 \cdot 6NH_3$ ; and  $g = 2.19 \pm 0.01$  and  $\theta = -1.50 \pm 0.1$  K for the  $Ni(BF_4)_2 \cdot 6NH_3$ . The  $g$ -factor for the  $Ni(ClO_4)_2 \cdot 6NH_3$  agrees with the previous determination of

Watanabe (14) but a significant discrepancy is found between our value of  $\theta$  and his ( $\theta = - 0.5$  K). This point will be discussed later.

Fig. 2 shows  $dM/dH$  versus  $T$  for  $H = 0$ , for temperatures below 2 K. For both salts a broad maximum marks the antiferromagnetic transition, followed by a decrease to about  $2/3$  of the peak value (powdered samples). The Néel temperature  $T_N$  corresponds to the point of maximum derivative (15) and numerical calculations of this derivative from the experimental points yield:  $T_N = 0.45$  K for the  $Ni(ClO_4)_2 \cdot 6NH_3$  and  $T_N = 0.43$  K for the  $Ni(BF_4)_2 \cdot 6NH_3$ .

Fig. 3 shows recordings of  $dM/dH$  versus  $H$  for two constant temperatures: 0.3 K (below  $T_N$ ) and 0.5 K (above but close to  $T_N$ ). For  $T < T_N$  two discontinuities are apparent, broadened, of course, due to the polycrystalline character of the samples. Just after the first discontinuity,  $dM/dH$  is approximately equal to the peak value in Fig. 2. This suggests that a spin-flop type of phenomenon occurs at this point, as has been observed in several other cubic antiferromagnetic materials (8,16). The second discontinuity should then mark the transition from the "canted" to the paramagnetic phases. Fig. 4 shows the position of these discontinuities in the  $H$ - $T$  plane, which should correspond to the magnetic phase diagram of the salts. The open circles in fig. 4 correspond to the position of a broad maximum observed for  $T \gtrsim T_N$ , a behavior that has already been reported for other compounds (17), and which is being presently studied in terms of correlation effects (18).

Assuming first-neighbor antiferromagnetic interaction

(in the molecular field approximation), the values of  $\theta$  obtained from our high temperature data, can be related to the  $T = 0$  canted-paramagnetic critical field  $H_c(0)$ , by:

$$H_c(0) \approx \frac{2k\theta}{g\mu_B} \quad (1)$$

Here we have neglected the influence of the anisotropy, which should be averaged out in our powdered samples. When the anisotropy is small compared to the exchange energy, its effect should be just the rounding of the peak at the transition and this is what is observed in fig. 3.

The above relation gives  $H_c(0) = 20.5$  kOe for the  $\text{Ni}(\text{ClO}_4)_2 \cdot 6\text{NH}_3$  and  $H_c(0) = 13.7$  kOe for the  $\text{Ni}(\text{BF}_4)_2 \cdot 6\text{NH}_3$ . These numbers are quite compatible with the portion of the phase boundaries shown in fig. 4.

On the other hand, the antiferro-canted critical field for  $T = 0$ ,  $H_{\text{SF}}(0)$ , is related to the anisotropy energy which in turn can be related to the splitting  $D$  of the  $\text{Ni}^{++}$  ground state. An estimate of  $H_{\text{SF}}(0)$  can be made remembering that  $H_{\text{SF}}$  is usually almost independent of  $T(19)$ , and so, from fig. 4, it is reasonable to take  $H_{\text{SF}}(0) \sim 4$  kOe for the  $\text{Ni}(\text{ClO}_4)_2 \cdot 6\text{NH}_3$ , and  $H_{\text{SF}}(0) \sim 5$  kOe for the  $\text{Ni}(\text{BF}_4)_2 \cdot 6\text{NH}_3$ .

The relation between  $H_{\text{SF}}(0)$  and  $D$  depends on the relative orientation of electrical axes, which, according to the point charge model of Bates and Stevens (4), can be any of the four equivalent  $\langle 111 \rangle$  crystallographic directions. It could be calculated with the assumption that, for instance, one fourth of the  $\text{Ni}^{++}$  ions would have its symmetry axis along each of the cube diagonals. To avoid this kind of complication, a ready

estimate of the order of magnitude of  $D$  can be made by means of Yosida's relation between the anisotropy energy and  $D$  for the uniaxial case (20), and the usual relation between the anisotropy energy and  $H_{SF}(0)$ . This yields:

$$D = \frac{g^2 \mu_B^2 H_{SF}^2(0)}{2k|\theta|} \quad (2)$$

Equation (2) results in  $D/k \sim 0.2$  K for both salts. This value is consistent with similar data reported for the isomorphous  $Ni(NO_3)_2 \cdot 6NH_3$  ( $(D/k) \sim 0.1$  K), and the values measured by EPR for all three halides ( $D/k = 0.4$  K).

The simplifying assumption of a uniaxial model certainly underestimates  $D$ . A more realistic calculation would lead to higher values, maybe by factors of 2 or 3. However, it would hardly change the order of magnitude of the presented value. Watanabe, based on a best-fit of zero-field susceptibility data above 1.2 K, reports  $D = 4.0 \text{ cm}^{-1}$  ( $(D/k = 5.6$  K) and  $\theta = -0.5$  K for the  $Ni(ClO_4)_2 \cdot 6NH_3$ . Such a high value of  $D$  is difficult to reconcile with the present data. Its sign, as presented by Watanabe, corresponds to the degenerate spin doublet lying lower in energy and this is consistent with our observation of an antiferromagnetic transition below 0.5 K. However, in this case, the curve of  $\chi_{\text{powder}}^{-1}$  versus  $T$  is rather insensitive to the parameter  $D$  and a best fit can easily lead to unrealistic values.

A less serious discrepancy exists also with respect to the parameter  $\theta$ . In favor of the value presented here, we point out the consistency of  $H_c(0)$ , calculated from (1), with the field dependence of  $dM/dH$  below  $T_N$  (as seen in fig. 4), and



also that our value of  $\theta$  is much closer to the molecular field prediction  $\theta = 3 T_N$  for an f.c.c. antiferromagnet where interactions with nearest neighbors are considered.

REFERENCES

1. PALMA-VITTORELLI M.B., PALMA M.U., DREWES G.W.J. and KOERTS W., *Physica* 26, 922 (1960).
2. CRZYBEK T., JANIK J.A., MAYER J., PYTASZ G., RACHWALSKA M. and WALUGA T., *Phys. Stat. Sol. (a)* 16, K165 (1973); and STANKOWSKI J., JANIK J.M., DEZOR A. and SCZANIECKI B., *Phys. Stat. Sol. (a)* 16, K167 (1973).
3. SCZANIECKI B., LARYS L. and GRUSZCZYNSKA U., *Acta Phys. Polon.*, A46, 759 (1974).
4. BATES A.R. and STEVENS K.W., *J. Phys. C* 2, 1573 (1969) and BATES A.R., *J. Phys. C* 3, 1825 (1970).
5. TRAPP C. and CHIN-I SHYR, *J. Chem. Phys.* 54, 196 (1971).
6. VAN KEMPEN H., DUFFY JR. W.T., MIEDEMA A.R. and HUISKAMP W. *Physica* 30, 1131 (1964).
7. BECERRA C.C., SANO W., MARQUES A., FROSSATTI G., PADUAN FILHO A., OLIVEIRA JR. N.F. and QUADROS C.J.A., *Phys. Letters* 40A, 203 (1972).
8. PADUAN FILHO A. and OLIVEIRA JR. N.F., *Phys. Lett.* 46A, 117 (1973).
9. OLIVEIRA JR. N.F. and QUADROS C.J.A., *Sol. State Comm.*, 7, 1531 (1969).
10. PADUAN FILHO A. and OLIVEIRA JR. N.F., *Sol. State Comm.* 15, 1167 (1974).
11. WYCKOFF R.W.G. - *The Structure of Crystals*, 19A, Supplement for 1930-1934 to the 2nd edition, Reinhold Publishing Corp., p. 85.
12. MAXWELL E. - *Rev. Sci. Instr.* 36, 553 (1965).
13. OLIVEIRA JR. N.F. and QUADROS C.J.A., *J. Sci. Instr. (J. Phys. E)*, 2, 967 (1969).
14. WATANABE T., *J. Phys. Soc. Japan* 16, 1131 (1961).
15. FISHER M.E., *Phylos. Mag.* 7, 1731 (1962).
16. OLIVEIRA JR. N.F., FONER S., SHAPIRA Y. and REED T.B., *Phys.*

- Rev. B 5, 2634 (1972).
17. METSELAAR J.W. and DE KLERK D., Physica 63, 191 (1973).
  18. FERREIRA L.G., private communication
  19. PADUAN FILHO A., BECERRA C.C., and OLIVEIRA JR. N.F., Phys. Letters 50A, 51 (1974).
  20. YOSIDA K., Prog. Theor. Phys. 6, 691 (1951).

FIGURE CAPTIONS

- Fig. 1 - Inverse of the Differential Magnetization (for  $H = 0$ ) as a function of  $T$ . The dashed lines correspond to the best-fit of the data above 2 K to a Curie-Weiss law. Note that the axis of  $(dM/dH)^{-1}$  for the  $Ni(ClO_4)_2 \cdot 6NH_3$  (left hand side) is displaced relative to the axis for  $Ni(BF_4)_2 \cdot 6NH_3$  (right hand side).
- Fig. 2 -  $dM/dH$  versus  $T$  below 2 K. The arrows indicate the Néel temperature determined by the point of largest derivative.
- Fig. 3 -  $dM/dH$  versus  $H$  at constant  $T$  for two temperatures: one below  $T_N$  and another just above  $T_N$  (dashed line). The arrows indicate the discontinuities plotted in fig. 4.
- Fig. 4 - Magnetic phase boundaries as determined from traces of  $dM/dH$  versus  $H$  at constant  $T$ . The arrows indicate: - the Néel temperature  $T_N$  as obtained in fig. 2; and the canted-paramagnetic critical field for  $T = 0$ ,  $H_c(0)$ , derived from the value of the Weiss temperature obtained in fig. 1. The open circles correspond to the positions of the broad maxima observed above  $T_N$ .

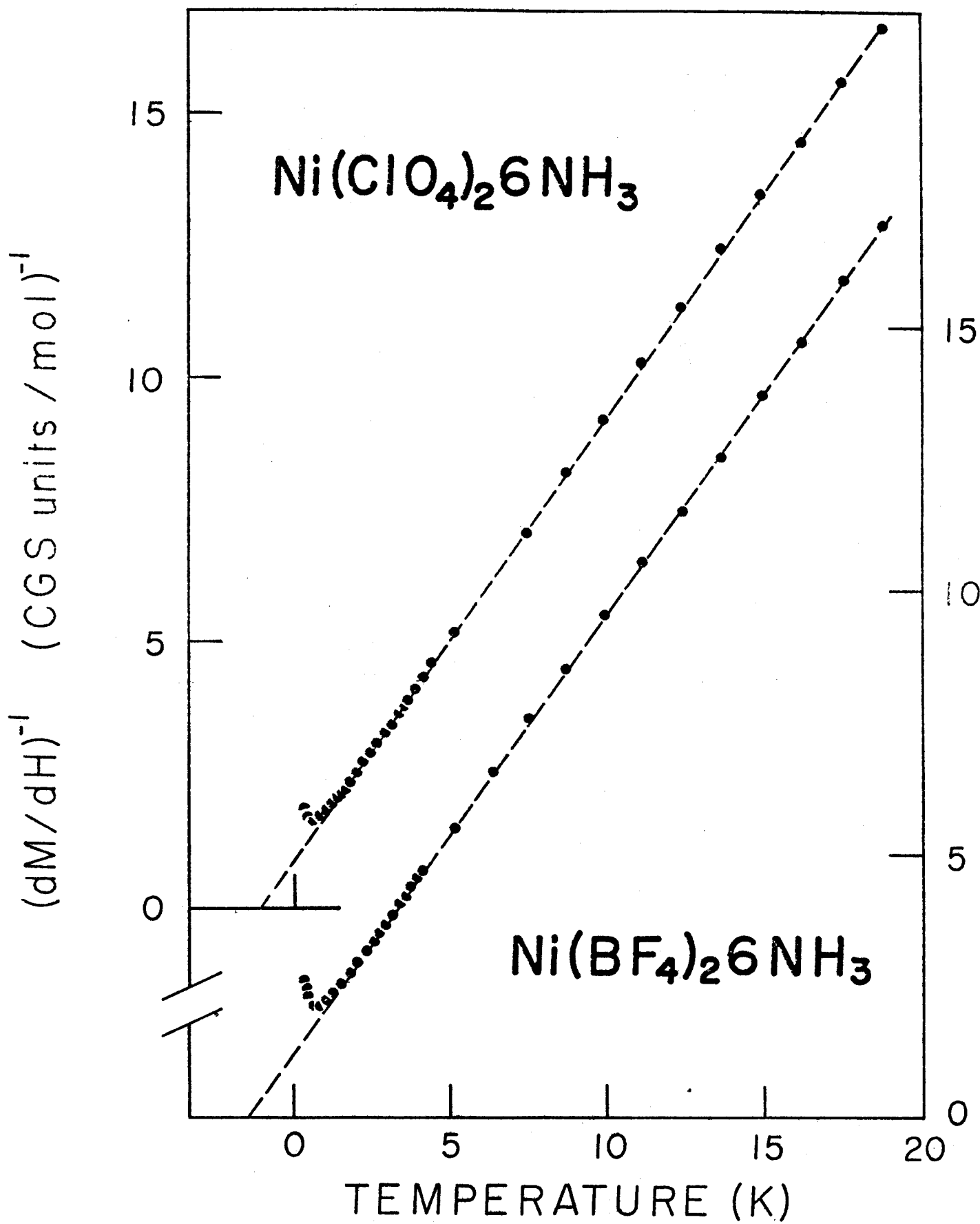


Fig. 1

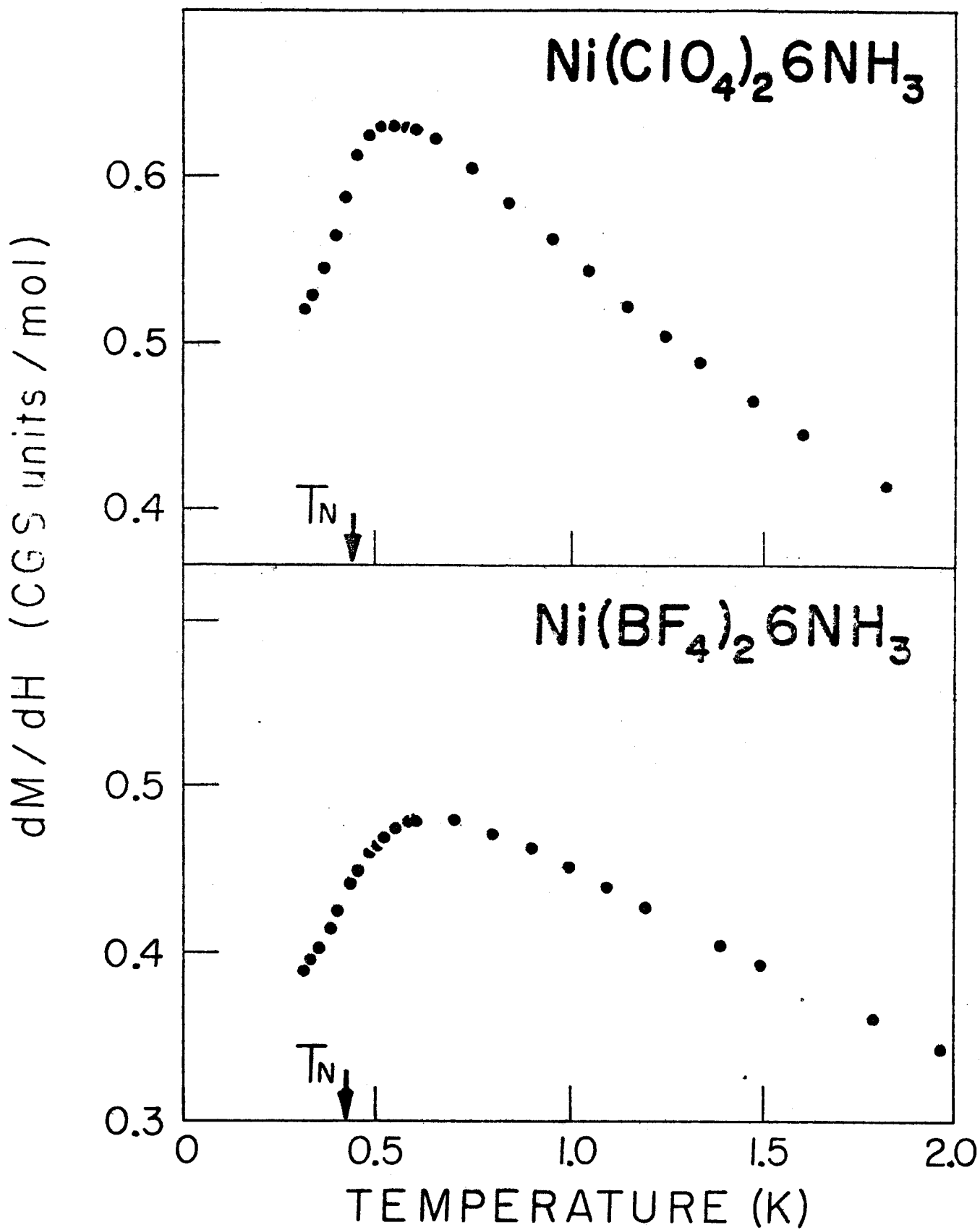


fig. 2

DIFFERENTIAL MAGNETIZATION (C.G.S. units/mol)

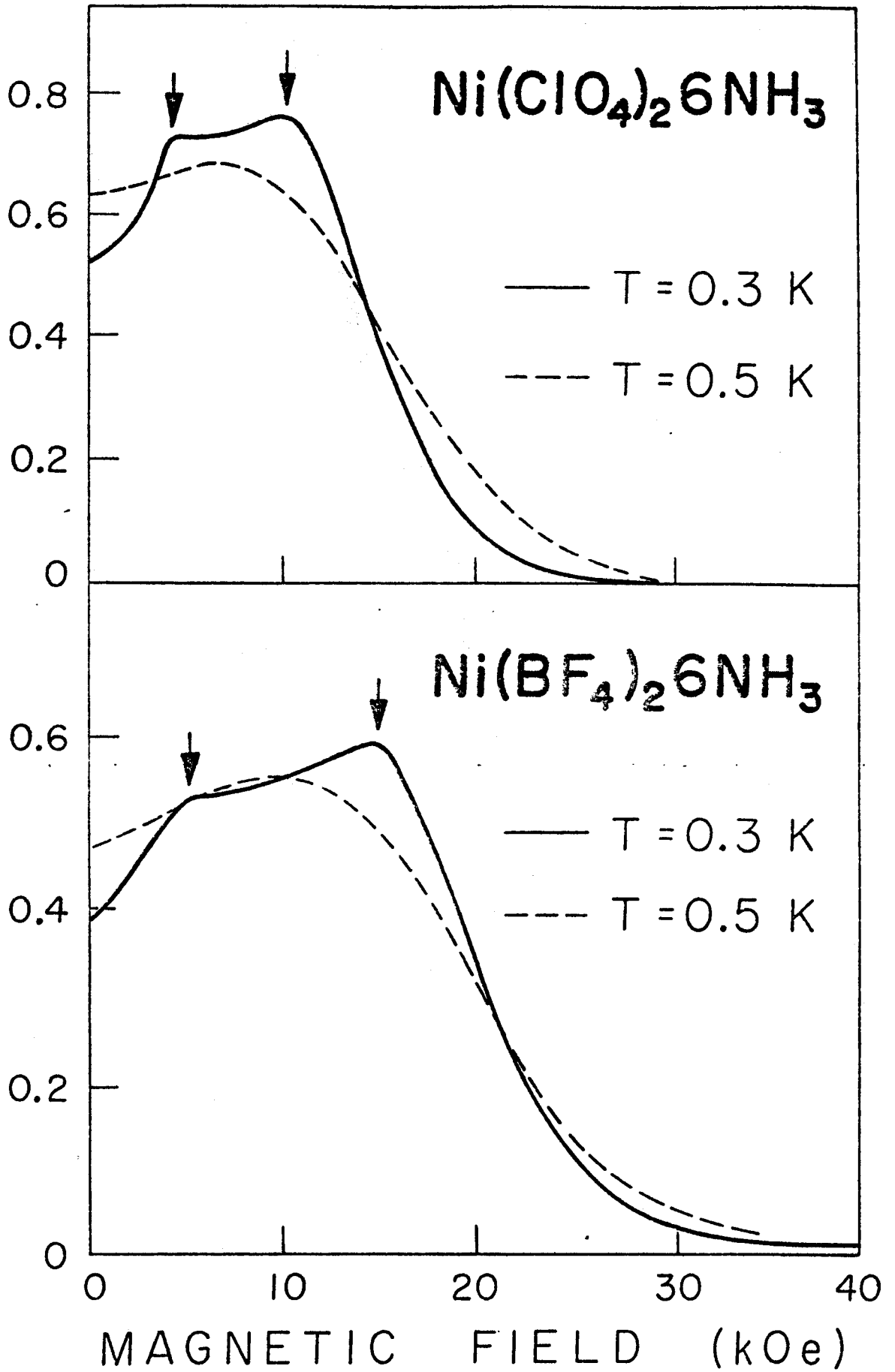


Fig. 3

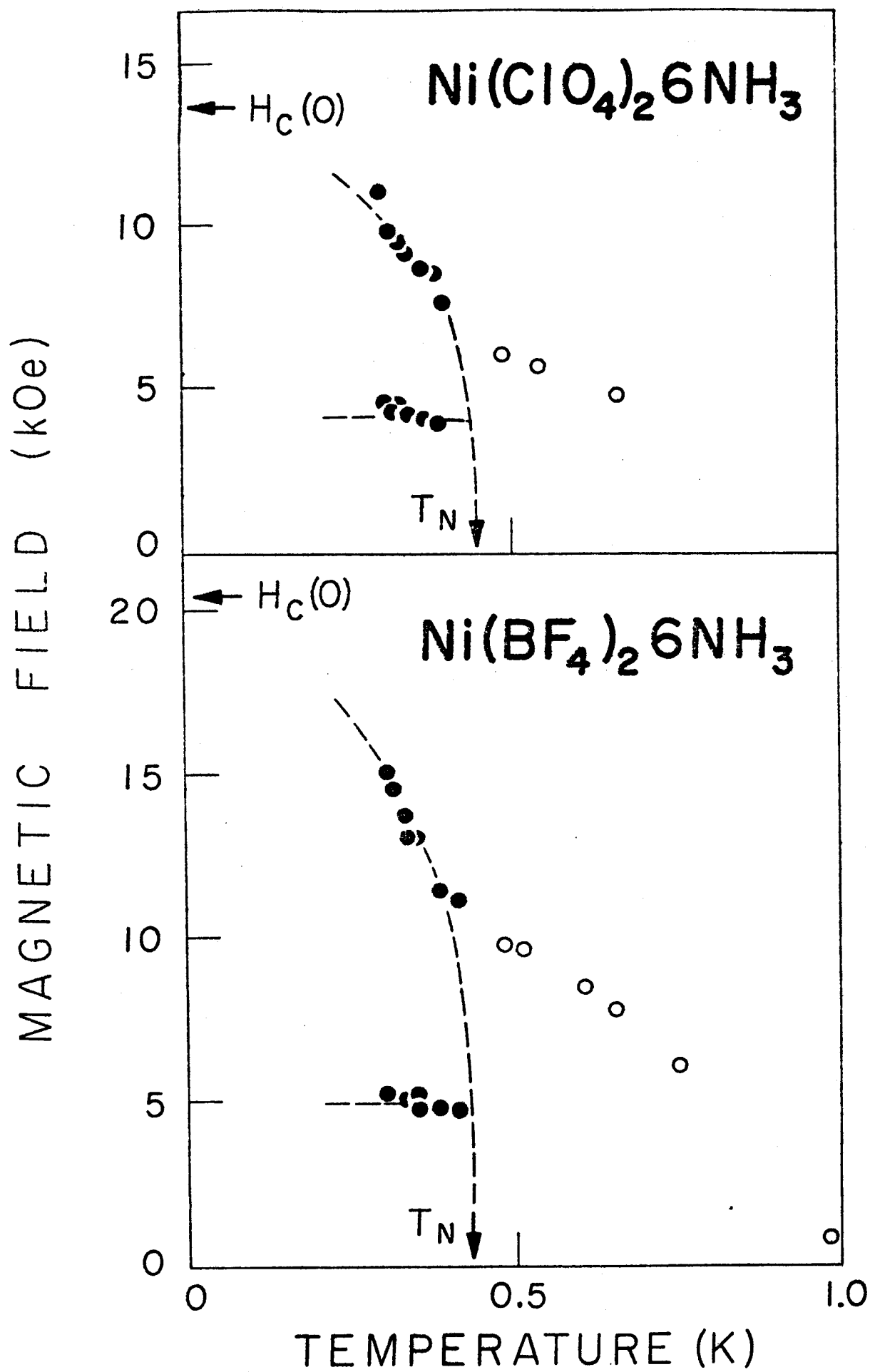


fig. 4